Electrochimica Acta 56 (2011) 2321–2327

Contents lists available at ScienceDirect

Electrochimica Acta

journal homepage: www.elsevier.com/locate/electacta

Characterization of the surface redox process of adsorbed morin at glassy carbon electrodes

Alvaro Yamil Tesio, Adrian Marcelo Granero, Héctor Fernández*, María Alicia Zón*

Departamento de Química, Facultad de Ciencias Exactas, Físico-Químicas y Naturales, Universidad Nacional de Río Cuarto, Agencia Postal N° 3, (5800) Río Cuarto, Argentina

ARTICLE INFO

Article history:
Received 25 August 2010
Received in revised form
10 November 2010
Accepted 11 November 2010
Available online 19 November 2010

Keywords:
Morin
Flavonoids
Cyclic voltammetry
Square wave voltammetry
Thermodynamic and kinetics parameters

ABSTRACT

The thermodynamic and kinetics of the adsorption of morin (MOR) on glassy carbon (GC) electrodes in 0.2 mol dm^{-3} phosphate buffer solutions (PBS, pH 7.00) was studied by both cyclic (CV) and square wave (SWV) voltammetries. The Frumkin adsorption isotherm was the best to describe the specific interaction of MOR with GC electrodes. The SWV allowed to characterize the thermodynamic and kinetics of surface quasi-reversible redox couple of MOR, using the combination of the "quasi-reversible maximum" and the "splitting of SW net peaks" methods. Average values obtained for the formal potential and the anodic transfer coefficient were (0.27 ± 0.02) V and (0.59 ± 0.09), respectively. Moreover, a value of formal rate constant (k_s) of 87 s^{-1} for the overall two-electron redox process was calculated. The SWV was also employed to generate calibration curves, which were linear in the range MOR bulk concentration (c^*_{MOR}) from 1.27×10^{-7} to 2.50×10^{-5} mol dm^{-3}. The lowest concentration experimentally measured for a signal to noise ratio of 3:1 was 1.25×10^{-8} mol dm^{-3} (3 ppb).

1. Introduction

Flavonoids are abundant in plants, and considered very important for preventing a wide variety of diseases, including, cardiovascular diseases, and allergies, certain forms of cancer, inflammations, and hepatic diseases [1]. Morin (MOR, Fig. 1), as a member of the family of the flavonols, has been shown to act as a potent antioxidant [2,3], xanthine oxidase inhibitor [4], cell proliferation inhibitor [5], apoptosis inducer [6], and modulator of lipoxygenase and cyclo-oxygenase activities in the arachidonic acid cascade [7]. MOR also acts as a chemopreventive agent against oral carcinogenesis *in vitro* and *in vivo* [8]. Furthermore, MOR exhibits inhibition of tetradecanoylphorbo-13-acetate-induced hepatocellular transformation [9]. MOR is a flavonol widely distributed in tea, coffee, and cereals as well as in a great variety of fruits and vegetables [10].

In our knowledge, there is very little information available in the literature concerning the electrochemical behavior of MOR [11]. Therefore, Wang et al. [11] studied the MOR electrochemical behavior on at glassy carbon (GC) electrodes in phosphate buffer solutions (PBS, pH 7.28) as well as the MOR interactions with DNA at modified GC electrodes with the poly(tetrafluoroethyl)-deoxyribonucleate acid. These authors found that the electrode process at GC electrodes had a diffusion/adsorption mixture control and from the slope and the intercept of peak potentials (E_p) vs. log v plots could infer that the global number of exchanged electron was $n = 2$.

The analysis of flavonoids has been carried out, principally, for thin-layer chromatography [12,13], gas chromatography [14,15], capillary electrophoresis [16–18], electrochemical measurements [19,20], high-performance liquid chromatography (HPLC) [21–25]. Specially, the chromatography HPLC has widely been used to separate and to analyze flavonoids.

In this work, we discuss the studies related to the thermodynamic and kinetics of the adsorption of MOR at GC electrodes in 0.2 mol dm^{-3} PBS (pH 7.00), where a surface quasi-reversible redox couple was obtained. The electrochemical techniques were the cyclic (CV) and square wave (SWV) voltammetries. The combination of the "quasi-reversible maximum" and the "splitting of the net SW voltammetric peak" methods [26–34] allowed obtaining information about the thermodynamic and kinetics of the overall superficial redox couples. The theory about the "quasi-reversible maximum" was initially developed assuming that there was no interaction between the immobilized species [26–33]. However, as this pre-requisite is not satisfied by virtually any experimental system, the theory that considers the case of surface reactions involving lateral interactions between adsorbed species has also been developed [33,34].

We have already studied the application of this methodology to carry out a full characterization of altertoxin I adsorbed at carbon paste electrodes [35] and both the redox coupled of cercosporin

* Corresponding authors.
E-mail addresses: atesio@exa.unrc.edu.ar (A.Y. Tesio), agranero@exa.unrc.edu.ar (A.M. Granero), hfernandez@exa.unrc.edu.ar (H. Fernández), azon@exa.unrc.edu.ar, alicia_zon@hotmail.com (M.A. Zón).

0013-4686/$ – see front matter © 2010 Published by Elsevier Ltd.
doi:10.1016/j.electacta.2010.11.037

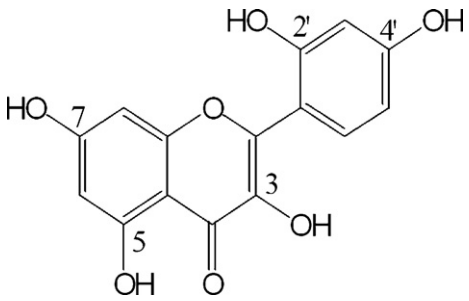

Fig. 1. Chemical structure of morin.

[36] and the ochratoxin A electro-oxidation product [37] adsorbed at GC electrodes.

2. Experimental

2.1. Reagents

MOR was from Sigma–Aldrich. MOR stock solutions (1×10^{-2} mol dm^{-3}) were prepared in ethanol (Sintorgan, HPLC grade) and kept in the refrigerator. They were stable for at least one month. Working solutions were prepared daily by adding aliquots of the stock solution to buffer solutions. The water was Sintorgan (HPLC grade). The PBS of pH 7.00 were prepared using 0.1 mol dm^{-3} Na_2PO_4H (Merck p.a.) and 0.1 mol dm^{-3} KPO_4H_2 (Merck p.a.). All reagents were used as received.

2.2. Apparatus and experimental measurements

CV and SWV experiments were performed with an AutoLab PGSTAT 12 potentiostat, controlled by GPES 4.9 electrochemical software from Eco-Chemie, Utrecht, The Netherlands. The variation of the scan rate (v) in CV measurements was from 0.050 to 1 V s^{-1}. For SWV, a square wave amplitude of ΔE_{SW} = 0.025 V and a staircase step height of ΔE_s = 0.005 V were mainly used. The frequency (f) varied from 10 to 500 Hz. In some experiments, ΔE_{SW} varied from 0.025 to 0.150 V. Electrochemical measurements were performed in a two compartment Pyrex cell [38]. The working electrode was a GC disk (BAS, 3 mm diameter), which was polished with 0.3 and then 0.05 μm wet alumina powder (from Fischer), copiously rinsed with water, and sonicated in a water bath for 5 min. Finally, it was transferred to a blank solution (PBS, pH 7.00) and cycled 10 times between 0 and 1 V. Very reproducible results were obtained when this pre-treatment was applied to the working electrode. The counter electrode was a large-area platinum foil (approximately 2 cm^2). The reference electrode was an aqueous saturated calomel electrode (SCE) fitted with a fine glass Luggin capillary containing a bridge solution identical to that containing the sample being measured.

The solutions were deareated by bubbling purified nitrogen for at least 10 min prior to measurement. The temperature was (25.0 ± 0.2) °C.

The fitting of experimental data using a nonlinear least squares procedure in the Origin 7.0 were performed to the effects of finding the best adsorption isotherm that describes the specific interaction of MOR with GC electrodes. We chose the best fitting between experimental and theoretical data when the Chi-square function (χ^2) was a minimum.

The pH measurements were performed with an Orion Model 720A pH-meter, calibrated daily with three commercial buffers.

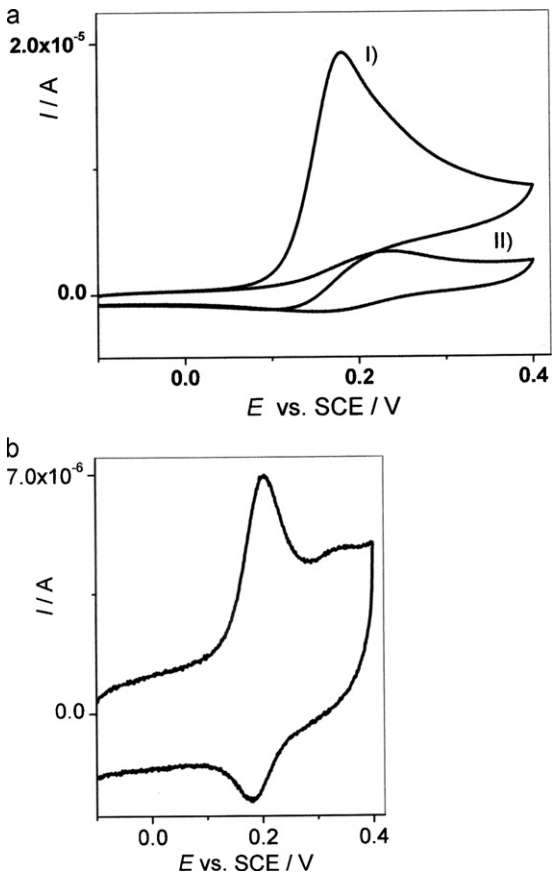

Fig. 2. a) Cyclic voltammograms recorded in the presence I) and II) in the absence of MOR ($c^*_{MOR} = 8.3 \times 10^{-4}$ mol dm^{-3}) in 0.2 mol dm^{-3} PBS (pH 7.00). v = 0.050 V s^{-1}. b) Cyclic voltammogram recorded in blank solution immediately after that the GC electrode was immersed during 180 s at a E_{acc} = −0.1 V in another solution formed by the same reaction medium but with a $c^*_{MOR} = 2.0 \times 10^{-5}$ mol dm^{-3}. v = 0.500 V s^{-1}.

3. Results and discussion

3.1. Cyclic voltammetry

Cyclic voltammograms registered for a solution of MOR in 0.2 mol dm^{-3} PBS (pH 7.00) in the potential range between −1.20 and 1.20 V showed two oxidation peaks. One well-defined centered at approximately 0.18 V and another poorly defined, centered at approximately 0.80 V. The first anodic peak can be assigned to the oxidation of −OH group presents in C3 while the second oxidation peak can be assigned to the oxidation of one of the −OH group presents in C2′, C4′, C5 or C7 in the MOR chemical structure (Fig. 1). Consecutive cyclic voltammograms registered in the potential range between −1.20 and 1.20 V showed a marked decrease in the current signals in successive sweeps. After the fifth successive sweep, voltammetric signals almost disappeared (results no shown). It is well known that the oxidation of phenols occurs in the potential range from 0.80 to 1 V depending of the reaction medium and might be represented, in principle, by an $E_1C_1E_2C_2$ mechanism generating, in some cases, polymeric products that poison or passive the working electrode surface of [39]. Based on these results, we only study in this work the electrochemical behavior of the first MOR oxidation peak.

Therefore, cyclic voltammograms recorded in 0.2 mol dm^{-3} PBS (pH 7.00) in the presence and in the absence of MOR at the same scan rate are shown in Fig. 2. Firstly, a cyclic voltammogram was recorded in a solution of MOR with a bulk concentration, $c^*_{MOR} = 8.3 \times 10^{-4}$ mol dm^{-3}. An oxidation peak, with an anodic potential

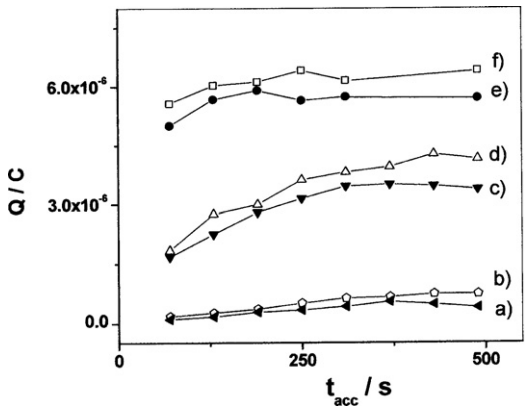

Fig. 3. Dependence of Q with t_{acc} obtained on a GC electrode ($A = 0.0707\ cm^2$). c^*_{MOR} a) 5×10^{-7}; b) 1×10^{-6}; c) 1×10^{-5}; d) 1×10^{-4}; e) 8.3×10^{-4} and f) 4×10^{-3} mol dm^{-3}. Composition of the reaction medium: 0.2 mol dm^{-3} PBS (pH 7.00). $\nu = 0.050$ V s^{-1}.

peak ($E_{p,a}$) at about 0.18 V was found during the first anodic scan (Fig. 2a, I). Any complementary cathodic peak was observed when the potential scan rate was reversed at low ν, putting clearly in evidence that chemical/s and/or electrochemical/s reactions are coupled to the initial electron transfer [40]. However, the corresponding complementary cathodic peak begins to define when v was increased to 0.500 V s^{-1}, showing a quasi-reversible behavior at $\nu = 1$ V s^{-1}. These findings clearly show that chemical/s and/or electrochemical/s reactions coupled to the initial charge transfer are relatively slow [40].

Then, the working electrode was immediately rinsed with the buffer solution and transferred to another electrochemical cell, which contained only the blank solution 0.2 mol dm^{-3} PBS (pH 7.00). The cyclic voltammogram recorded under this experimental condition also showed an oxidation peak with smaller currents and shifted at slightly more positive potentials (Fig. 2a, II) than that obtained previously in the presence of MOR. These results put clearly in evidence the adsorption of MOR at GC electrode surface as well as the main MOR oxidation peak shows a diffusion/adsorption mixture control.

Preferential accumulation of the reactant or product, or the adsorption of both on the electrode surface can be also inferred from the cyclic voltammograms obtained after transferring the electrode with the accumulated flavonoid to a blank solution (Fig. 2b) (see below).

Experiments performed on the voltammetric peak centered about at 0.18 V by using different accumulation times (t_{acc}) showed an increase in the $I_{p,a}$, which evidenced clearly the surface nature for this electrochemical signal. On the basis of these results, studies were conducted to find the most favorable accumulation time (t_{acc}) as well as the optimum accumulation potential (E_{acc}) for performing the MOR pre-concentration step at the electrode surface. The best E_{acc} was −0.1 V vs. SCE. On the other hand, stationary currents were achieved at $t_{acc} = 180$ s as it can be observed from plots of charge (Q) vs. t_{acc} (Fig. 3).

Therefore, a cyclic voltammogram recorded in a blank solution immediately after that the GC electrode was immersed for 180 s at an $E_{acc} = -0.1$ V in another solution formed by the same reaction medium but with a $c^*_{MOR} = 2.0 \times 10^{-5}$ mol dm^{-3} is shown in Fig. 2b. An average value for potential at $1/2 I_{p,a}$, called half-peak potential ($E_{p/2}$) of (0.068 ± 0.0001) was obtained, being this value slightly greater than the theoretical expected for a two-electron transfer, i.e., $E_{p/2} = 0.045$ V [40]. Moreover, the separation between the anodic and cathodic peak potentials (ΔE_p) was of 0.020 V. These results clearly suggest both the adsorption of MOR at GC electrodes as well as the quasi-reversible nature of the surface redox reaction considering the characteristic of cyclic voltammograms. Reproducibility of the quasi-reversible signal showed in Fig. 2b was obtained in blank solutions at low c^*_{MOR} and $\nu \geq 0.500$ V s^{-1}. These results are in a very good agreement with those theoretically predicted [40].

The area under the oxidation peak, corrected for any residual charging current, represents the charge associated with the oxidation of adsorbed MOR, i.e., $Q = nFA\Gamma_{MOR}$, where n is the number of exchanged electrons per mole of oxidized substance, F is the Faraday constant, A is the electrode area and Γ_{MOR} is the surface concentration of MOR adsorbed [40]. An average value of $\Gamma_{MOR} = (4 \pm 1) \times 10^{-12}$ mol cm^{-2} was determined in the scan rate range from 0.025 to 0.075 V s^{-1}, which would correspond to a submonolayer of MOR adsorbed [40].

These findings show a selective interaction of MOR with the carbon surface. In principle, the explication of this behavior could be considering that several oxygen containing functional groups, such as carboxylic acid, lactone, *o*-quinone, *p*-quinone, carbonyl, phenol, etc., may be present on a GC surface [41]. The interaction between these functional groups and –OH, ether and C=O groups present in the chemical structure of MOR (Fig. 1) might be responsible for the adsorption of MOR on GC electrodes.

The adsorption isotherm derived from the dependence between c^*_{MOR} and the fractional coverage of the electrode surface (θ) was studied. The surface coverage was defined as $\theta = I_p/I_{p,max}$ (or Q/Q_{max}), where I_p and Q are the peak current and charge, respectively, from cyclic voltammograms obtained at a given t_{acc} for different c^*_{MOR}. $I_{p,max}$ and Q_{max} are maximum values of I_p and Q obtained at the same t_{acc} at the greatest c^*_{MOR} studied. As can be observed in Fig. 4a, the Q_{max} was reached at $c^*_{MOR} \geq 5 \times 10^{-5}$ mol dm^{-3} for $t_{acc} = 180$ s and $E_{acc} = -0.1$ V. A plot of c^*_{MOR} against θ is shown in Fig. 4b. The experimental results were fitting for finding the best adsorption isotherm which describes the specific interaction of MOR with GC electrodes. The best fitting was found when the Frumkin adsorption isotherm [40] was chosen to perform the fit (Fig. 4b). Therefore, the expression of the Frumkin adsorption isotherm is [40]:

$$\beta c^*_{MOR} = \frac{\theta}{1-\theta} \exp^{-g'\theta} \quad (1)$$

where $g' = 2g\Gamma_{MOR}/RT$ is the parameter characterizing the interaction between the adsorbed species, Γ_{MOR} and c^*_{MOR} were previously defined and $\beta = \exp(-\Delta G_{ads}/RT)$ is the adsorption coefficient [40,42]. The Frumkin adsorption isotherm can provide a useful insight into lateral interactions that may exist within these monolayers since it models the free energy of adsorption as an exponential function of the surface coverage.

The fit was performed for values of $0.2 < \theta < 0.9$. For the best fit, average values of $\beta = (3.7 \pm 0.2) \times 10^4$, $g' = (1.90 \pm 0.08)$ and $\chi^2 = 9.7 \times 10^{-14}$ were obtained. There is a very good agreement between experimental data and the results of this fit. A value of $\Delta G_{ads} = -26.1$ kJ mol^{-1} was obtained for the standard free energy of adsorption. This indicates that the overall adsorption process of MOR molecules onto the GC surface is energetically favorable. In addition, a positive value for g' indicates that interactions between neighboring adsorbed species on the electrode surface are attractive [40].

3.2. Square wave voltammetry

SW voltammograms are highly sensitive to the charge transfer kinetics of surface redox processes [26,27,33]. It is well known that the combination of the methods of the "quasi-reversible maximum" and the "splitting of the net voltammetric peak" [28,29] can be used to calculate the formal rate constant (k_s), the transfer coefficient ($1-\alpha$) and the formal potential ($E^{0'}_f$) of redox couples immobilized on the electrode surface [28–33]. The quasi-reversible

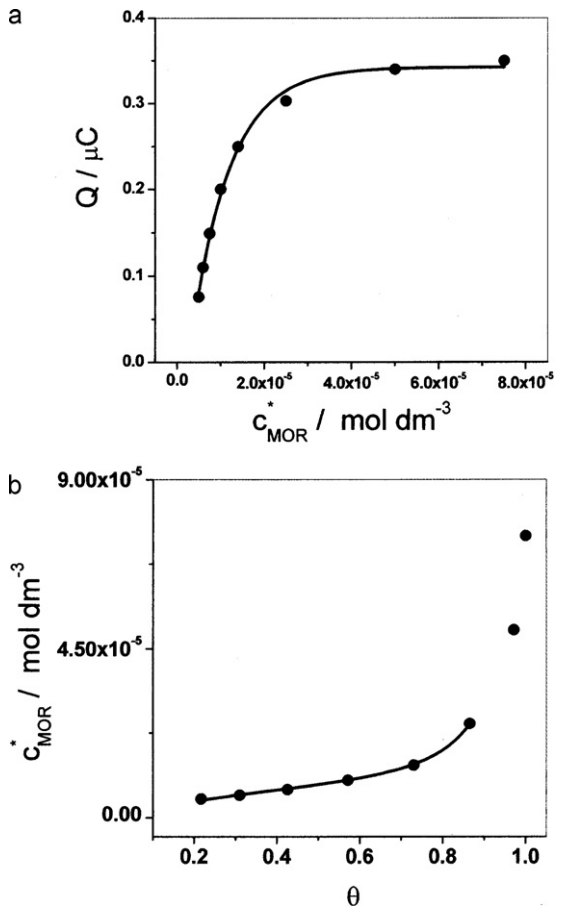

Fig. 4. a) Dependence of Q with c^*_{MOR}. The reaction medium: 0.2 mol dm^{-3} PBS (pH 7.00) and v = 0.050 V s^{-1}. b) Morin bulk concentrations vs. the electrode surface saturation coverage. Experimental data compared with the best-fit Frumkin adsorption isotherm. (●) Indicate experimental points and (–) indicates the best-fit line.

maximum method predicts that the ratio between the net peak current ($I_{p,n}$) and the frequency is approximated as a parabolic function of the dimensionless kinetic parameter, ω, defined as the ratio between the standard (formal) rate constant (k_s) and the frequency. The splitting of the net voltammetric peak occurs when the SW amplitude is increased at a given frequency. This methodology was used to carry out a full thermodynamic and kinetics characterization of the MOR surface redox couple at GC electrodes in 0.2 mol dm^{-3} PBS (pH 7.00).

Forward (I_f), reverse (I_r) and net (I_n) currents obtained from SW voltammograms of MOR adsorbed on GC electrodes after transferring the electrode to a blank solution (0.2 mol dm^{-3} PBS, pH 7.00) are shown in Fig. 5. They present a strong evidence of the surface quasi-reversible nature of this electrochemical signal [33].

The apparent reversibility of the confined redox reaction at the electrode surface depends on the kinetics parameter, ω. Net peak currents from these SW voltammograms are linearly proportional to the frequency, but the factor of this proportionality is a function of the reaction reversibility. If the adsorptions of both the reactant and the product of a quasi-reversible redox couple are equally strong, a maximum appears in the plot of $I_{p,n}f^{-1}$ vs. f or f^{-1}, at a SW frequency which is approximately equal to k_s of the redox reaction [27,33]. In the region of the maximum, the curve can be approximated by a parabola, and if $(I_{p,n}f^{-1}) = (I_{p,n}f^{-1})_{max}$, then $f_{max} = k_s/\omega_{max}$ [33]. Thus, the equation:

$$k_s = \omega_{max} f_{max} \quad (2)$$

is a convenient way to calculate k_s.

Table 1
Dependence of the maximum frequency with the accumulation time and the concentration of MOR in the accumulation solution. ΔE_{SW} = 0.025 V; ΔE_s = 0.005 V.

$10^6 c^*_{MOR}$ (mol dm^{-3})	t_{acc} (s)	θ	f_{max} (s^{-1})	$k_{s,app}$ (s^{-1})[a]
1	180	0.077	76	68
5	180	0.217	50	45
5	120	0.140	64	58
5	60	0.080	77	69
7.5	180	0.426	45	40
10	180	0.571	44	39

[a] $k_{s,app} = f_{max}\omega_{max}$, where ω_{max} = 0.9 was obtained from Table 2.3 of Ref. [33] for $n\Delta E_{SW}$ = 0.050 V and $(1-\alpha)$ = 0.6.

Moreover, the theory predicts that a useful "quasi-reversible maximum" appears only if $-1.5 < \log\omega < 1.5$ [34].

The theoretically calculated critical kinetics parameter, ω_{max}, depends on the transfer coefficient $(1-\alpha)$, on the product of the SW amplitude and the number of electrons, $n\Delta E_{SW}$, but it is independent of the normalized potential increment, $n\Delta E_s$ and of the amount of initially adsorbed reactant [33]. In the presence of uniform lateral interactions between adsorbed species, the product of the real standard rate constant, k_s and the exponential term $\exp(-2g'\theta)$ defines a new apparent rate constant of the surface redox reaction:

$$k_{s,app} = k_s \exp(-2g'\theta) \quad (3)$$

where $g'\theta$ is the interaction product. Therefore, the degree of interactions depends on both the relative coverage of the electrode surface θ and Frumkin interaction parameter g' [33,34]. The position of the maximum is associated with a certain critical value of the interaction product $(g'\theta)_{max}$, which depends on the value of the ratio k_s/f. Therefore, to reach the quasi-reversible maximum, the following condition must be satisfied:

$$k_s \exp^{-2(g'\theta)} f_{max}^{-1} = (\omega_{int})_{max} \quad (4)$$

where the values of $(\omega_{int})_{max}$ are identical with ω_{max} for a simple surface redox reaction without interactions between adsorbed species. Moreover, as $k_{s,app} = k_s \exp(-2g'\theta)$, it is possible to infer that when the interaction forces are attractive ($g' > 0$) the formal rate constant for the surface redox couple decreases.

Plots of $I_{p,n}f^{-1}$ vs. f obtained as previously described after MOR accumulation onto the GC electrode are shown in Fig. 6. These plots obtained a different t_{acc} (at a given c^*_{MOR}) as well as at different c^*_{MOR} (at t_{acc} = 180 s) are shown in Figs. 6a–c, respectively. As it can be observed, the f_{max} decreases with both the t_{acc} and the c^*_{MOR} as it is theoretically expected for a surface redox couple with attractive interactions between adsorbed molecules [33] (see Table 1).

The theory also predicts that if the rate of reaction becomes rapid, the net peak current of a SW voltammogram splits and the net peak height approaches zero [28]. The skew of forward and reverse peaks on the potential scale, as the dimensionless rate constant is increased, produced the splitting of the net peak. Experimentally, we can find this behavior when the SW frequency decreasing or the SW amplitude is increased [28]. However, changes in the peak shape, which carry kinetics information, are more efficiently producing the variation of the SW amplitude than the frequency [28]. Thus, a set of SWV experiments where, c^*_{MOR} and the SW amplitude was varied at a given frequency was performed. The net, forward, and reverse currents recorded at a frequency of 100 Hz and at different ΔE_{SW} are shown in Fig. 5. As is theoretically predicted [28,29,33], large changes in voltammogram shape are obtained when ΔE_{SW} increases for an appropriate fixed frequency. For small ΔE_{SW} (i.e., 0.025 V) and f = 100 Hz, a single net peak is observed. However, at the same frequency the peak started to split at about ΔE_{SW} = 0.050 V and is almost completely split at ΔE_{SW} = 0.125 V.

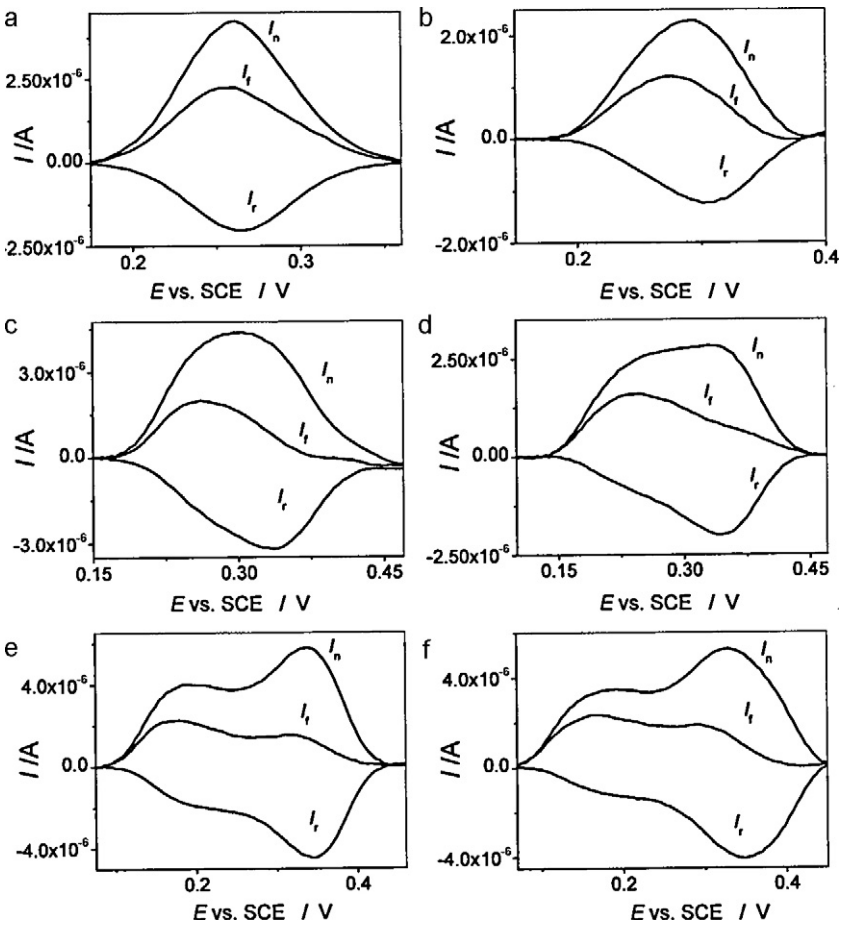

Fig. 5. The forward (I_f), reverse (I_r) and net (I_n) currents from SW voltammograms of MOR adsorbed on a GC electrode, recorded in blank solution 0.2 mol dm^{-3} PBS (pH 7.00) at different SW amplitudes. ΔE_{SW} were a) 0.025 V, b) 0.050 V, c) 0.075 d) 0.100 e) 0.125 V and f) 0.150 V. The c^*_{MOR} in the accumulation solution was 1×10^{-5} mol dm^{-3}. Other SWV parameters were $\Delta E_s = 0.005$ V and $f = 100$ Hz.

An average value for the formal potential of the surface redox couple of $\overline{E_f^{0'}} = (0.27 \pm 0.02)$ V was obtained from $E_f^{0'} = \frac{1}{2}(E_{p,a} + E_{p,c})$, where $E_{p,c}$ and $E_{p,c}$ are the peak potentials for anodic (forward) and cathodic (reverse) scans, respectively.

On the other hand, for $(1-\alpha) > 0.2$, the ratio between the anodic (forward) and cathodic (reverse) peak currents, $I_{p,a}/I_{p,c}$ can be approximated by a single exponential curve [33]:

$$\frac{I_{p,a}}{I_{p,c}} = 5.5414 \exp[-3.4606(1-\alpha)] \quad (5)$$

From Eq. (5) an average value of $\overline{(1-\alpha)} = (0.59 \pm 0.09)$ was calculated.

Experimental values of $E_{p,a}$, $E_{p,c}$, $I_{p,a}$, $I_{p,c}$, the ratio between $I_{p,a}$ and $I_{p,c}$ and $(1-\alpha)$ for the MOR overall two-electron oxidation are shown in Table 2.

Values of $k_{s,app}$ were calculated from Eq. (2) using the values of ω_{max} obtained from Table 2.3 in Ref. [33] (see Table 1), i.e., 0.9 for $n\Delta E_{SW} = 0.050$ V and $(1-\alpha) = 0.6$ (Table 1). The error in the estimation of $k_{s,app}$ by using ω_{max} is close to 10% [33].

A plot of $\ln k_{s,app}$ vs. θ (Eq. (3)) was linear in the range $0.080 < \theta < 0.217$ (four points were included in the correlation, $r = 0.9975$). From the intercept and the slope of this plot, values of (1.51 ± 0.07) and 87 s^{-1} were calculated for the Frumkin interaction parameter and the overall formal rate constant, respectively. The value of g' is close to that previously determined from CV measurements ($g' = 1.90$).

3.3. Determination of MOR in pure solutions

Some results of MOR adsorbed SWV responses with the MOR bulk concentration are studied here as a simple introduction for a future publication about its analytical application. The net current–potential curve in SWV is the most useful analytical signal [33]. The high sensitivity of the adsorptive accumulation method is obviously the greatest advantage.

Besides, the adsorptive accumulation is analytically useful only if the portion of the electrode surface covered by the adsorbed reactant is small (about 20% of the total area). Under this condition, the relationship between the surface concentration of the adsorbed substrate and its bulk concentration may be considered as approx-

Table 2
Anodic ($E_{p,a}$) and cathodic ($E_{p,c}$) peak potentials (vs. SCE), anodic ($I_{p,a}$) and cathodic ($I_{p,c}$) peak currents for the split SW peaks, the ratio between $I_{p,a}$ and $I_{p,c}$, $(1-\alpha)$ and $E_f^{0'}$ values for the overall two-electron adsorbed redox couple at GC electrodes in 0.2 mol dm^{-3} buffer phosphate pH 7.00 aqueous solutions. $\Delta E_s = 0.005$ V and $f = 100$ Hz. The concentration of MOR in the accumulation solution was $c^*_{MOR} = 1 \times 10^{-5}$ mol dm^{-3}.

ΔE_{SW}	$E_{p,a}$ (V)	$I_{p,a}$ (μA)	$E_{p,c}$ (V)	$-I_{p,c}$ (μA)	$I_{p,a}/I_{p,c}$	$(1-\alpha)$	$E_f^{0'}$ (V)
0.025	0.256	2.265	0.261	2.034	1.114	0.46	0.258
0.050	0.276	1.265	0.300	1.240	0.972	0.51	0.288
0.075	0.261	1.991	0.335	3.201	0.630	0.63	0.298
0.100	0.252	1.593	0.344	1.998	0.797	0.56	0.298
0.125	0.164	2.262	0.345	4.491	0.504	0.70	0.254
0.150	0.169	2.273	0.344	4.056	0.560	0.66	0.256

$\overline{E_f^{0'}} = (0.27 \pm 0.02)$ V; $\overline{(1-\alpha)} = (0.59 \pm 0.09)$.

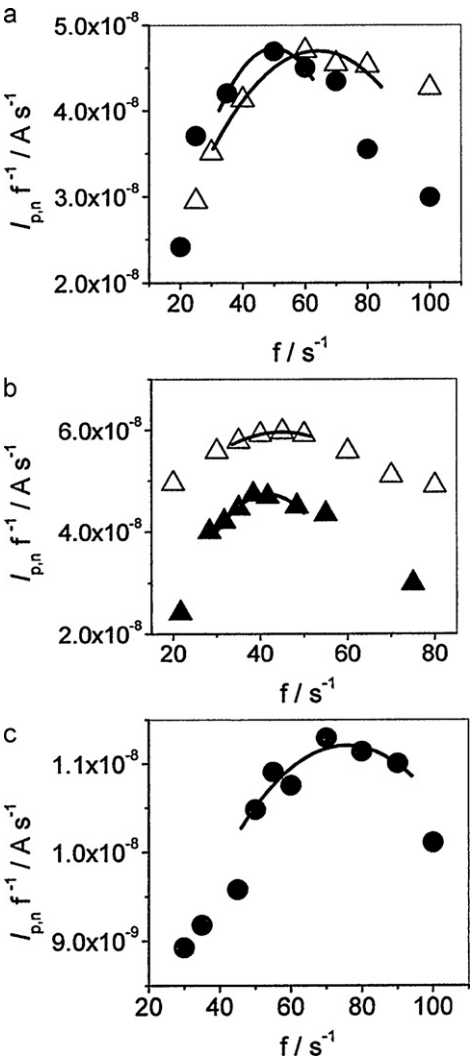

Fig. 6. Dependence of the ratio of net peak current and frequency ($I_{p,n}f^{-1}$) and the SW frequency obtained for MOR in the reaction medium 0.2 mol dm^{-3} phosphate buffer solution (pH 7.00). a) t_{acc}: △ = 120 s; ● = 180 s ($c^*_{MOR} = 5 \times 10^{-6}$ mol dm^{-3}). b) c^*_{MOR}: ▲= 7.5×10^{-6} mol dm^{-3} and △ = 10×10^{-6} mol dm^{-3} (t_{acc} = 180 s). c) ● c^*_{MOR} = 1×10^{-6} mol dm^{-3} (t_{acc} = 180 s). f_{max} was calculated from the first derivative of the mathematical expression for the parabola resulting from a best fit with experimental $I_{p,n}f^{-1}$ values. ΔE_{SW} = 0.025 V and ΔE_s = 0.005 V.

imately linear [27]. The combination of adsorptive accumulation with SWV provides to be an electroanalytical tool very valuable for performing trace analysis of compounds that are both surface active and electroactive. The determination of MOR was carried out in blank unstirred solutions (0.2 mol dm^{-3} PBS, pH 7.00) after performing its accumulation at the GC electrode surface in solutions of different c^*_{MOR} during t_{acc} = 180 s at E_{acc} = −0.10 V. A linear relationship between $I_{p,n}$ vs. c^*_{MOR} was obtained at f = 100 Hz in the range from 1.27×10^{-7} to 2.50×10^{-5} mol dm^{-3}. The linear regression can be expressed by a least square procedure as:

$$I_{p,n} = (0.39 \pm 0.01) \times c^*_{MOR} - (1.1 \pm 0.1) \times 10^{-8}, \quad r = 0.9998 \quad (6)$$

In Eq. (6), $I_{p,n}$ is expressed in amperes and c^*_{MOR} in mol dm^{-3}. Data used in the regression analysis of the calibration plot were the average of three replicated measurements (eight experimental points were taken into account).

In addition, the lowest concentration value measured experimentally for a signal to noise ratio of 3:1 [37] was 1.25×10^{-8} mol dm^{-3} (3 ppb).

4. Conclusions

It has been shown that the adsorption of MOR on GC electrodes, under experimental conditions where the reaction is mainly controlled by the reactant adsorption, follows the Frumkin adsorption isotherm. In addition, attractive interactions between adsorbed molecules characterize the adsorption process.

The combination of the "quasi-reversible maximum" and the "split of net SW peaks" methods, where the interaction between adsorbed molecules was taken into account, was employed for the first time to carry out a full thermodynamic and kinetics characterization of morin adsorbed at glassy carbon electrodes. On the other hand, the adsorptive accumulation of morin at glassy carbon electrodes appears as a very promising analytical tool for the determination of morin in the future in real samples.

Acknowledgements

Financial support from Consejo Nacional de Investigaciones Científicas y Técnicas (CONICET) and Secretaría de Ciencia y Técnica (SECyT) from the Universidad Nacional de Río Cuarto is gratefully acknowledged.

A.Y. Tesio and A.M. Granero thank a doctoral and a post-doctoral fellowship, respectively, from Consejo Nacional de Investigaciones Científicas y Técnicas (CONICET), Argentina.

References

[1] J.E. Middleton, C. Kandaswami, T.C. Theoharides, Pharmacol. Rev. 52 (2000) 673.
[2] T.W. Wu, L.H. Zeng, J. Wu, K.P. Fung, Life Sci. 53 (1993) 213.
[3] T.W. Wu, L.H. Zeng, J. Wu, K.P. Fung, Biochem. Pharmacol. 47 (1994) 1099.
[4] Z. Yu, W.P. Fong, C.H. Cheng, J. Pharmacol. Exp. Ther. 316 (2006) 169.
[5] H.M. Kuo, L.S. Chang, Y.L. Lin, H.F. Lu, J.S. Yang, J.H. Lee JH, Anticancer Res. 27 (2007) 395.
[6] S.K. Manna, R.S. Aggarwal, G. Sethi, B.B. Aggarwal, G.T. Ramesh, Clin. Cancer Res. 13 (2007) 2290.
[7] M.J. Laughton, P.J. Evans, M.A. Moroney, J.R. Hoult, B. Halliwell, Biochem. Pharmacol. 42 (1991) 1673.
[8] K. Kawabata, T. Tanaka, S. Honjo, M. Kakumoto, A. Hara, H. Makital, Int. J. Cancer 83 (1999) 381.
[9] C.Y. Hsiang, S.L. Wu, T.Y. Ho, Biochem. Pharmacol. 69 (2005) 1603.
[10] J. Kuhnau, World Rev. Nutr. Diet 24 (1976) 117.
[11] F. Wang, Y. Xu, J. Zhao, S. Hu, Bioelectrochemistry 70 (2007) 356.
[12] H. Vogel, M. Gonzalez, F. Fainic, I. Razmilic, J. Rodriguez, J.S. Martin, F. Urbina, J. Ethnopharmacol. 97 (2005) 97.
[13] X.F. Yang, F. Wang, S.S. Hu, Colloid Surface B 52 (2006) 8.
[14] Y.C. Fiamegos, C.G. Nanos, J. Vervoort, C.D. Stalikas, J. Chromatogr. A 1041 (2004) 11.
[15] C. Proestos, I.S. Boziaris, G.J.E. Nychas, M. Komaitis, Food Chem. 95 (2006) 664.
[16] X.Q. Xu, H.Z. Ye, W. Wang, L.S. Yu, G.N. Chen, Talanta 68 (2006) 759.
[17] X.Q. Xu, L.S. Yu, G.N. Chen, J. Pharm. Biomed. Anal. 41 (2006) 493.
[18] T. Wu, Y.Q. Guan, J.N. Ye, Food Chem. 100 (2007) 1573.
[19] S. Ignatov, D. Shishniashvili, B. Ge, F.W. Scheller, F. Lisdat, Biosens. Bioelectron. 17 (2002) 191.
[20] A. Doménech-Carbo, M.T. Doménech-Carbo, M.C. Saurí-Peris, Talanta 66 (2005) 769.
[21] B. Liu, D. Anderson, D.R. Ferry, L.W. Seymour, P.G. de Takats, D.J. Kerr, J. Chromatogr. B 666 (1995) 149.
[22] U. Justesen, P. Knuthsen, T. Leth, J. Chromatogr. A 79 (1998) 101.
[23] H.F. Wang, K.H. Well, Food Res. Int. 34 (2001) 223.
[24] F. Fang, J.M. Li, Q.H. Pan, W.D. Huang, Food Chem. 101 (2007) 428.
[25] C.S. Lau, D.J. Carrier, R.R. Beitle, D.I. Bransby, L.R. Howard, J.O. Lay Jr., R. Liyanage, E.C. Clausen, Bioresource Technol. 98 (2007) 429.
[26] M. Lovric, S. Komorsky-Lovric, J. Electroanal. Chem. 248 (1988) 239.
[27] S. Komorsky-Lovric, M. Lovric, Fresenius Z. Anal. Chem. 335 (1989) 289.
[28] J.J. OïDea, J.G. Osteryoung, Anal. Chem. 65 (1993) 3090.
[29] S. Komorsky-Lovric, M. Lovric, Electrochim. Acta 40 (1995) 1781.
[30] V. Mirceski, M. Lovric, Electroanalysis 11 (1999) 984.
[31] V. Mirceski, R. Gulaboski, B. Jordanoski, S. Komorski-Lovric, J. Electroanal. Chem. 490 (2000) 37.
[32] F. Garay, V. Solis, J. Electroanal. Chem. 505 (2001) 109.
[33] V. Mirceski, S. Komorsky-Lovric, M. Lovric, Square Wave Voltammetry. Theory and Application, Springer, Leipzig, Germany, 2007.
[34] V. Mirceski, M. Lovric, R. Gulaboski, J. Electroanal. Chem. 515 (2001) 91.
[35] P.G. Molina, M.A. Zón, H. Fernández, Electroanalysis 12 (2000) 791.

[36] N.C. Marchiando, M.A. Zón, H. Fernández, Electroanalysis 15 (2003) 40.
[37] E.A. Ramírez, M.A. Zón, P.A. Jara Ulloa, J.A. Squella, L. Nuñez Vergara, H. Fernández, Electrochim. Acta 55 (2010) 771.
[38] H. Fernández, M.A. Zón, J. Electroanal. Chem. 322 (1992) 237.
[39] O. Hammerich, B. Svensmark, in: H. Lund, M.M. Baizer (Eds.), Organic Electrochemistry: An Introduction and a Guide, 3rd ed., Marcel Dekker, Inc, New York, 1990, p. 616.
[40] A.J. Bard, L.R. Faulkner, Electrochemical Methods: Fundamentals and Applications, 2nd ed., Marcel Dekker, New York, 2001.
[41] R.L. McCreery, in: A.J. Bard (Ed.), Carbon Electrodes: Structural Effects on Electron Transfer Kinetics in Electroanalytical Chemistry, 17, Marcel Dekker, New York, 1991, pp. 221–274.
[42] J. Lyklema, Fundamentals of Interface and Colloid Science, vol. 2, Academic Press, London, 1995.